Vol. 44, No. 4 (2022) 652-663, DOI: 10.24874/ti.1337.07.22.10

Tribology in Industry

www.tribology.rs

RESEARCH

Preparation and Tribological Properties of TiO_2/WO_3 Nanocomposite Lubricant

Xiaomeng Zhang[a], Qinjian Du[a], Sang Xiong[a,b,*], Cheng Peng[a]

[a]*College of Materials Science and Engineering, Nanjing Institute of Technology, Nanjing Jiang Su, P.R China,*
[b]*Jiangsu Key Laboratory of Advanced structural Materials and Application Technology, Nanjing Jiang Su, P.R China.*

Keywords:

Nanocomposite
Lubricants
TiO_2
Tribology
Lubrication mechanism

* Corresponding author:

Sang Xiong
E-mail: xiongsang@njit.edu.cn

Received: 20 July 2022
Revised: 7 September 2022
Accepted: 8 October 2022

A B S T R A C T

Nanocomposite Lubricants have been the focus of research in recent years. In this paper, tetrabutyl titanate (TBOT) was used to obtain TiO_2-encapsulated WO_3 nanoparticles, their microstructures and morphology were characterized by XRD and SEM. Adsorption site and interaction energy of citric acid, triethanolamine oleate, stearic acid and trioctyl phosphate as dispersants and TiO_2 were calculated. The results demonstrate that the reactivity from strong to weak follow the order of citric acid > triethanolamine oleate > stearic acid > trioctyl phosphate. Among the four dispersants, triethanolamine oleate has the strongest electron gain and loss ability and adsorption capacity and used as dispersant to obtain TiO_2/WO_3 nanocomposite lubricant. Addition of 0.015 vol.% TBOT, the oil film strength is up to 530 N and COF is 0.087. The lubrication mechanism of the TiO_2/WO_3 nano composite in the sliding process is attribute to tribofilm lubrication.

1. INTRODUCTION

Friction and wear are an important cause of equipment failure and low production efficiency in modern industrial production [1,2]. Reducing friction and wear is the primary task to improve the service life of equipment, improve production efficiency and reduce capacity loss [3,4]. Lubricant is one of the important means to reduce friction and wear [5,6].

Lubricants consist of base oil and additives. Additives can be divided into conventional organic molecules, two-dimensional layered, nano metal oxides [6-9] etc. Two-dimensional MoS_2, H-BN graphite and WS_2 are considered to be effective lubricating additives [10-12]. It is mainly due to its unique structure, large specific surface area, strong stiffness and weak interlayer interaction [13,14]. Graphene-based nano-materials are widely used as lubrication additives due to they are easy to shear and relatively smooth [13-15]. Fluorinated graphene has excellent thermal and chemical stability, good mechanical strength, and larger layer spacing than graphene [16,17]. Metal and carbon-based nanoparticles are used to reduce friction and resist wear [12,18-21]. Metal oxide nanoparticles, such as TiO_2, SiO_2, Al_2O_3 and ZnO, can be used as microball bearings rolling in the contact interface region, as abrasives with

polishing effects on worn surfaces, or as third bodies providing surface repair effects [22-25]. Softer metal nanoparticles [26-28], such as Ag and Cu, have been shown to form a tribofilm at the interface, which exhibit low shear stress and reduce the wear rate of steel-steel contacts. Hard carbon-based nanoparticles [29-30], such as diamond, can be considered for ball rolling or for increasing surface hardness through contact with the surface. Soft carbon-based nanoparticles, such as graphite and fullerenes [31-33], can be combined to form a protective film on the contact surface, thus effectively protecting the friction pair [34,35].

The main methods for preparing nanocomposites include sol-gel method, interlayer insertion method, blending method, in-situ dispersion polymerization, radiation synthesis method, template method [36], self-assembly method [37], molecular deposition film method, etc. [38]. The friction and wear characteristics of nano-composites are not only related to the composition structure of the composites, but also closely related to the external experimental conditions [39]. Zhao *et al*. [40] prepared TiO_2/ F-RGO nanocomposites by in-situ composite method and studied the influence of load on tribological properties of TiO_2/ F-RGO nanocomposites. Meng *et al*. [41] and Hu *et al*. [42] showed that nano-composites improved the friction and wear properties. Liu *et al*. [43] prepared Au/TiO_2 nanocomposite films by sol-gel method, and studied the tribological properties of Au/TiO_2 nanocomposite films when grinding with AISI52100 steel balls. Kasiarova *et al*. [44] and Bhimaraj P *et al*. [45] found that relative humidity and crystallinity are also important factors affecting the friction and wear properties of nanocomposites in some cases. In previous studies, TiO_2/WO_3 nanocomposite particles were not synthesized, and the influence of nanomaterial characteristics on collaborative lubrication behavior was not studied.

In this paper, WO_3 nanoparticles prepared by the sol-gel method and TiO_2/WO_3 nanocomposite particles prepared by hydrolysis process of tetrabutyl titanate (TBOT), their microstructures and morphology were characterized by XRD and SEM. The adsorption sites and interaction energies between citric acid, triethanolamine oleate, stearic acid and trioctyl phosphate and TiO_2 were theoretically calculated. The tribological behavior of the prepared nanoparticles and dispersants in the base fluid was studied by four-ball friction testing machine, and the wear surface of the nanoparticles was observed, the wear and friction mechanism of nanoparticles as anti-wear additives between metal friction pairs is proposed.

2.EXPERIMENTAL SECTION

2.1 Raw materials

The raw materials used in the preparation of TiO_2/WO_3 nanoparticles are europium(III.) hexahydrate ($Eu(NO_3)_2{\cdot}6H_2O$), ammonium paratungstate ($(NH_4)\ 10H_2(W_2O_7)6xH_2O$), citric acid monohydrate ($C_6H_8O_7{\cdot}H_2O$), acetonitrile (C_2H_3N), tetrabutyl titanate (TBOT) ($C_{16}H_{36}O_4Ti$), absolute ethanol (C_2H_6O), ammonia (NH_4OH), etc. The raw materials used in the preparation of the lubricant are glycerin ($C_3H_8O_3$, thickener to improve the viscosity of the fluid, moisturizer to prevent volatilization, purchased from Shanghai McLean Biochemical Technology Co., Ltd.), polyethylene glycol ($HO(CH_2CH_2O)$ nH, to increase fluid viscosity, as a humectant), triethanolamine ($C_6H_{15}NO_3$, preparation of oleic acid triethanolamine), oleic acid ($C_{18}H_{34}O_2$, preparation of oleic acid triethanolamine). Except for glycerol, all are purchased from Sinopharm Chemical Reagent Co., Ltd.

2.2 Selection and calculation of dispersants

Materials studio software with Dmol3 module was used to calculate the chemical parameters of the alternative dispersant, the molecular frontier orbital energy of the dispersants was calculated first, and the molecular activity of the chemical reaction of the dispersant was analyzed. Then the adsorption energy of the dispersant on the preferred crystal surface of the nanoparticles was calculated, and the appropriate dispersant by the size of the adsorption energy was selected. Four dispersants in common, including stearic acid ($C_{18}H_{36}O_2$), citric acid ($C_6H_8O_7$), triethanolamine oleate ($C_{24}H_{47}NO_4$) and trioctyl phosphate ($C_{24}H_{51}O_4P$), were used and the chemical parameters of the above four dispersants were calculated to select the most suitable dispersant. Melting point and density of four dispersants were tested according to GB T 617-2006 and GB4472-84, the details of the four dispersants selected are shown in Table 1.

Table 1. Details of four dispersants for the test.

Dispersants	Chemical formula	Functional group	Melting point (℃)	Density(gcm^{-3})
Stearic acid	$C_{18}H_{36}O_2$	carboxyl	70	0.84
Citric acid	$C_6H_8O_7$	carboxyl	156	1.542
Triethanolamine oleate	$C_{24}H_{47}NO_4$	carbonyl	-18	0.96
Trioctyl phosphate	$C_{24}H_{51}O_4P$	Phosphate group	-70	0.92

2.3 Preparation and characterization of TiO_2/WO_3 nanoparticles

WO_3 nanoparticles are prepared by the sol-gel method, and then nano-TiO_2 is coated on its surface to obtain TiO_2/WO_3 nanocomposites in our previous work [46]. Three TiO_2/WO_3 samples were prepared by the various concentrations of TBOT (0.01 vol.%, 0.015 vol.% and 0.02 vol.%). The structure of the prepared TiO_2/WO_3 nanocomposite particles was characterized by X-ray diffraction pattern, and the microscopic morphology and size of the TiO_2/WO_3 nanocomposite particles were characterized by scanning electron microscopy (SEM) and transmission electron microscope (TEM).

2.4 Preparation of nano-lubricants

Triethanolamine oleate was selected as a dispersant, glycerol and polyethylene glycol were used to increase the viscosity of the fluid. Lubricant consists of TiO_2/WO_3 nanoparticles (0.1wt%), glycerol (5wt%), oleic acid (1.5wt%) and triethanolamine (1.5wt%). After selecting the test reagent, the nanoparticles are pre-dispersed as follows. 100ml of deionized water was added to the beaker, 5 ml of glycerol and 0.1 g of the prepared WO_3 nanoparticles was add them to the beaker, stirred with a magnetic stirrer for stirring for 30 min. 50ml of deionized water, triethanolamine and oleic acid were added to the beaker in turn, with a constant temperature magnetic stirrer and heated to 80 °C for 30 min. After stirring, it was cooled to room temperature, then added to a beaker containing pre-dispersed solution and stirred for 15 min.

2.5 Friction and wear properties of lubricants

Tribological properties of the TiO_2/WO_3 nanocomposite fluid were studied using the MR-S10A four ball tribometer. The maximum non-jamming load (P_B) of the nanofluid is measured to reflect the carrying capacity of the nanoparticle lubrication film. The P_B value was determined by the 10 s test according to GB/T3142-2019, and the rotation speed of the upper steel ball was 1450 r/min. Long-term wear test was conducted according to NB/SH/T0189-2017. The coefficient of friction (μ) and the diameter of the wear scars (D) are measured, and their worn morphology are analyzed.

3. RESULTS AND ANALYSIS

3.1 TiO_2/WO_3 nanoparticle characterization

The XRD pattern of TiO_2/WO_3 and WO_3 nanoparticles prepared at pH=10 is shown in Fig.1. The pattern of WO_3 is consistent with the ICDD/JCPDS PDF #71-2142 card. Then, the phases of TiO_2/WO_3 are found to be basically consistent with the PDF standard cards of PDF #71-2142 and PDF #72-0784. The prepared TiO_2/WO_3 sample has a strong diffraction peak at (002), (020), (200), (202), (-202), (400), (402), (402), and its unit cell constant is a=7.313Å, b=7.525Å, c=7.689Å, α=β=γ=90°. The diffraction peak of TiO_2 phases are detected at (101), (004), (200) and (105).

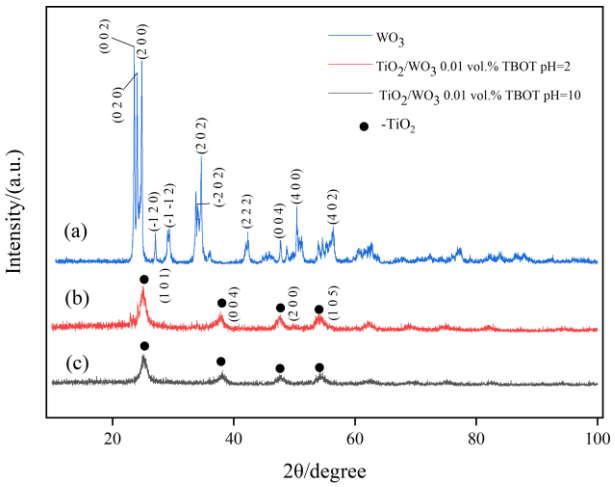

Fig. 1. XRD diagram of WO_3 nanoparticles, TiO_2/WO_3 nanocomposite particles prepared under alkaline condition (pH=10) and acidic condition (pH=2).

Grain size and full width at half maximum (FWHM) of TiO_2/WO_3 composite material are

obtained by adding different concentrations of TBOT (0.01 vol.%, 0.015 vol.%) were calculated using Scherrer formula as follow,

$$D = \frac{K\lambda}{\beta \cos\theta} \quad (1)$$

where K is *Scherrer* constant (k=1), D is the grain size (nm), β is FWHM.

According to Scherrer formula, the and shown in Fig.2. The black line is FWHM, and the blue line is the grain size. It can be concluded that the prepared TiO_2/WO_3 composite by adding 0.01 vol.% TBOT has the largest grain size under acidic condition, while the prepared TiO_2/WO_3 composite by adding 0.01vol.% TBOT has the smallest grain size under alkaline condition, and their half-width is inversely proportional to the grain size.

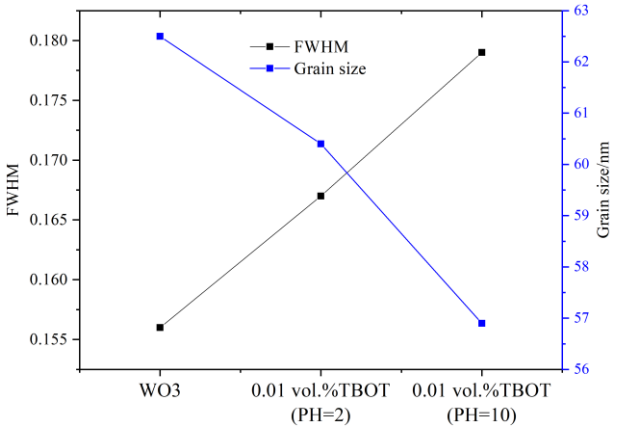

Fig. 2. FWHM and grain size of WO_3 nanoparticles, TiO_2/WO_3 nanocomposite particles.

he microscopic morphology of TiO_2/WO_3 nanocomposite particles is shown in Fig. 3. As can be seen from Fig. 3, TiO_2/WO_3 nanocomposite particles are spherical, and the nanoparticles prepared under acidic conditions (Fig. 3b, d) are all show high-density agglomeration structures, while the surface of the nanoparticles prepared under alkaline conditions (Fig. 3a, c) is relatively loose. It can be seen that the nanoparticles prepared under acidic conditions have a larger particle size (~50nm) than that of alkaline condition (~20 nm). According to the research results of Bhimaraj P *et al*. [45], when the particle size of nanoparticle is smaller, the anti-wear and anti-friction properties of the prepared lubricant is better. Therefore, it can be speculated that lubricant containing nanoparticles prepared under alkaline conditions has better tribological properties.

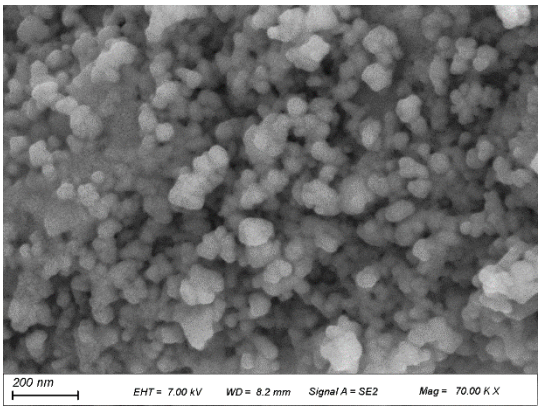

(a)

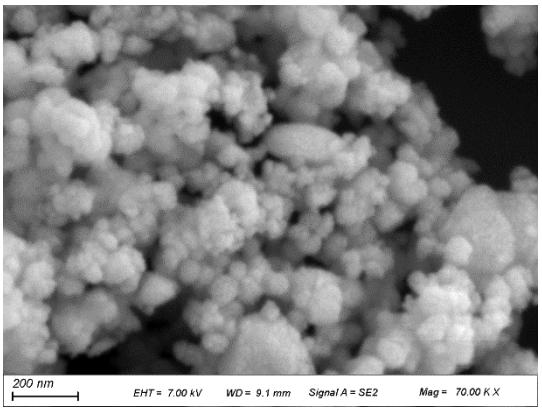

(b)

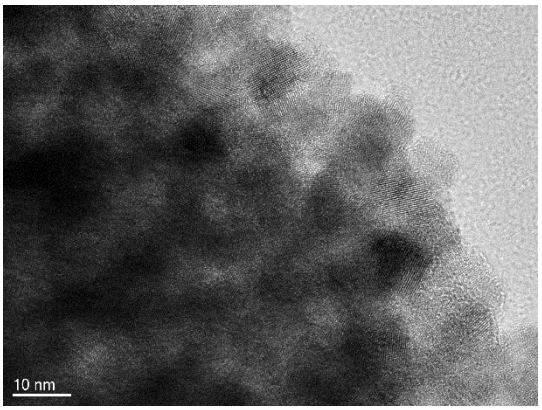

(c)

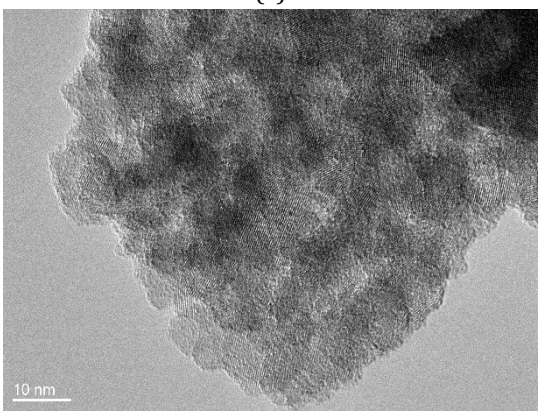

(d)

Fig. 3. SEM and HTEM images of TiO_2/WO_3 nanoparticles prepared under alkaline condition (a, c) and acidic condition (b, d).

3.2 Calculation of dispersants

Based on molecular orbital theory, the quantum chemical parameters of four dispersants of stearic acid ($C_{18}H_{36}O_2$), citric acid ($C_6H_8O_7$), triethanolamine oleate ($C_{24}H_{47}NO_4$) and trioctyl phosphate ($C_{24}H_{51}O_4P$) were calculated by using the Dmol3 module of Materials studio, and the calculation results of the highest occupied orbital energy (E_{HOMO}) and the lowest unoccupied orbital energy (E_{LUMO}) are shown in Table 2. The higher the value of E_{HOMO} indicates that the stronger the ability of the molecule to give electrons, the lower the value of E_{LUMO} indicates that the stronger the ability of the molecule to obtain electrons, and the smaller the energy gap (ΔE = E_{LUMO}-E_{HOMO}) value, the higher the reactivity of the molecule.The calculated the hardness (η), electrophilic index (ω), softness (S) and chemical potential (μ) and other chemical parameters of the molecule are shown in Table 3. The larger values of ω and S indicate that the molecules are more easily adsorbed. The smaller η is, the stronger adsorption capacity is. The quantum chemical parameters of the molecule are calculated using the following formula:

$$\eta = \frac{1}{2}\left(E_{LUMO} - E_{HOMO}\right) \tag{2}$$

$$S = \frac{1}{\eta} = \left(\frac{\partial \mu}{\partial N}\right)_v \tag{3}$$

$$\mu = \frac{1}{2}\left(E_{HOMO} + E_{LUMO}\right) \tag{4}$$

$$\omega = \frac{\mu^2}{\eta} \tag{5}$$

The reactivity of the four dispersants follows the order of citric acid> triethanolamine oleate> stearic acid > trioctyl phosphate. In addition, it can be seen that trioctyl phosphate has a low ability to give electrons, but its ability to accept electrons is strong. The ability of citric acid to gain and lose electrons is weak. The electron gain-loss capacity of triethanolamine oleate is the strongest of the four dispersants chosen. Among the four dispersants, the E_{HOMO} value of triethanolamine oleate is significantly lower than that of the other three dispersants, and the electron donor capacity of the other three dispersants was similar. The E_{LUMO} value of trioctyl phosphate was the lowest, indicating that it had the strongest ability to accept electrons. Citric acid has the highest E_{LUMO} value, indicating that it is the least electron receptive.

Fig. 4 demonstrates the optimized molecular configurations, HOMO, and LUMO of the four dispersants under an aqueous solvent. The HOMO and LUMO of citric acid and triethanolamine oleate are mainly distributed on carbonyl and carboxyl groups. In order to further determine the ability of these dispersants to gain and lose electrons during the reaction, the Fukui index of four dispersants in aqueous solvents was calculated theoretically, and the results are shown in Table 3.

$$f_k^+ = q_k(N+1) - q_k(N) \tag{6}$$

$$f_k^- = q_k(N) - q_k(N-1) \tag{7}$$

Where f_k^- represents the electrophilic index, f_k^+ nucleophilic index, and f_k^0 represents the free radical index. In electrophilic reactions, atoms are easy to lose electrons, so they have high value of f_k^-, while in nucleophilic reactions, on the contrary, atoms are easy to gain electrons, so they have high value of f_k^+. In free radical reactions, atoms form bonds by forming a common electron pair, so it has a high value of f_k^0.

Table 2. Chemical parameters of four dispersants.

Molecules	E_{HOMO} (eV)	E_{LUMO} (eV)	ΔE(eV)	η(eV)	μ(eV)	S(eV^{-1})	ω(eV)
$C_{18}H_{36}O_2$	-6.594	-1.044	5.550	-3.819	0.360	2.775	5.256
$C_6H_8O_7$	-6.699	-2.941	3.758	-4.820	0.532	1.879	12.364
$C_{24}H_{47}NO_4$	-5.783	-0.674	5.109	-3.229	0.391	2.555	4.080
$C_{24}H_{51}O_4P$	-6.821	0.486	7.307	-3.168	0.274	3.654	2.746

Table 3. Fukui indices of four dispersants under water solvent conditions.

Chemical formula	Functional group	Partial atomic number	Atom	f_k^-(a.u.)	f_k^+(a.u.)	f_k^0(a.u.)
$C_6H_8O_7$	carboxyl	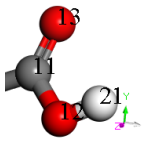	C(11)	0.047	0.091	0.069
			O(12)	0.051	0.060	0.055
			O(13)	0.145	0.125	0.135
			H(21)	0.033	0.039	0.036
$C_{24}H_{51}O_4P$	Phosphate group	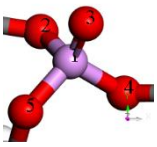	P(1)	0.027	0.113	0.070
			O(2)	0.052	-0.003	0.025
			O(3)	0.092	0.009	0.050
			O(4)	0.033	-0.013	0.010
			O(5)	0.041	-0.018	0.012
$C_{24}H_{47}NO_4$	carbonyl	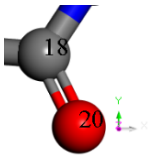	C(18)	0.035	0.145	0.090
			O(20)	0.114	0.112	0.113
$C_{18}H_{36}O_2$	carboxyl	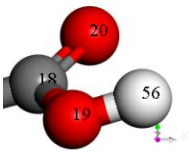	C(18)	0.049	0.304	0.176
			O(19)	0.040	0.129	0.084
			O(20)	0.163	0.231	0.197
			H(56)	0.025	0.066	0.045

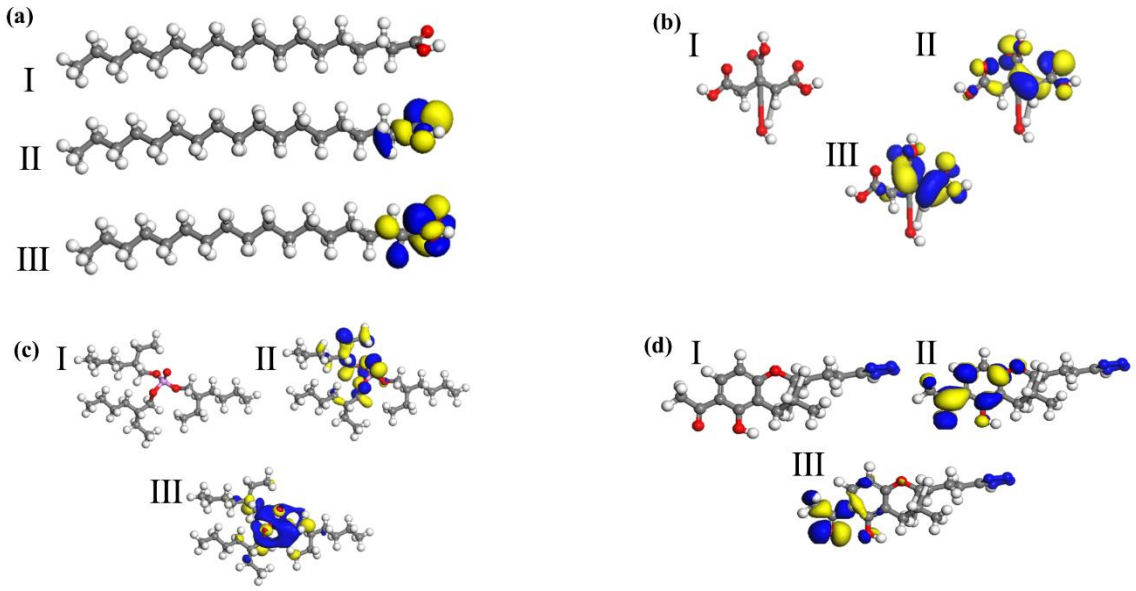

Fig. 4. Optimized molecular configuration, (II) HOMO, (III) LUMO of the four dispersants (a) stearic acid, (b) citric acid, (c) trioctyl phosphate, (d) triethanolamine oleate.

As can be seen from Table 3, for carboxyl compounds such as citric acid and stearic acid, oxygen atoms in carboxyl groups have strong ability to donate and accept electrons in both electrophilic reactions and nuclear reactions. For the phosphate compound trioctyl phosphate, the oxygen atom of the phosphate group in the electrophilic reaction has a stronger ability to give electrons, and the carbon atom of the phosphate group in the nucleophilic reaction has a stronger ability to receive electrons, while the oxygen atom is weak in receiving electrons. the carbonyl oxygen atom in the electrophilic reaction has a strong ability to donate electrons, and the carbonyl carbon atom in the nucleophilic reaction has a strong ability to receive electrons.

Molecular dynamics calculations were carried out using the FORCITES module in materials studio software, and the adsorption energy of the four dispersants on the TiO_2 (0 0 2) crystal plane was calculated and selected as the optimal dispersant. According to the law of conservation of energy, the adsorption energy (E_{Ads}) between TiO_2 and the dispersant is calculated using Equation (8).

$$E_{ads} = E_{total} - E_{mol} - E_{suf} \quad (8)$$

where, E_{Mol} is the energy of isolated surface modifier molecules, eV. E_{Surf} is the energy on the surface of nanoparticles when the modifier molecules are not adsorbed, eV. E_{Tot} is the total energy of surface modifier molecules and nanoparticles, eV.

The model changes before and after adsorption are shown in Fig. 5. As can be seen from Table 4, the adsorption energy of triethanolamine oleate and stearic acid is negative, mainly provided by non-bonding energy, which belongs to physical adsorption. The adsorption energy of trioctyl phosphate and citric acid is positive, mainly provided by bond energy, which belongs to chemical adsorption. The calculated adsorption energy of citric acid, stearic acid, triethanolamine oleate and trioctyl phosphate in the aqueous solvent are 6.180 eV, -14.022 eV, -13.612 eV and 10.954 eV respectively. Although, the adsorption energy of stearic acid was slightly higher than others, stearic acid was insoluble in water, triethanolamine oleate is selected as the dispersant for this test.

Table 4. Adsorption energy of dispersant molecules on the surface of nanoparticles.

Molecules	energy	E_{Ads}(eV)	E_{Tot}(eV)	E_{Mol}(eV)	E_{Surf}(eV)
$C_{18}H_{36}O_2$	sum	-14.022	-76848.241	-39.911	-76794.309
	Bond Energy	1.630	-20.828	-22.457	0.000
	Non-bonded Energy	-15.651	-76827.413	-17.453	-76794.309
$C_6H_8O_7$	sum	6.180	-76817.098	-28.970	-76794.309
	Bond Energy	13.030	16.699	3.669	0.000
	Non - bond energy	-6.850	-76833.797	-32.639	-76794.309
$C_{24}H_{47}NO_4$	sum	-13.612	-76815.412	-7.492	-76794.309
	Bond Energy	3.086	-16.429	-19.516	0.000
	Non - bond energy	-16.698	-76798.983	12.024	-76794.309
$C_{24}H_{51}O_4P$	sum	10.954	-76783.328	9.319	-76794.309
	Bond Energy	23.782	23.808	8.507	0.000
	Non - bond energy	-12.828	-76807.136	0.812	-76794.309

3.3 Tribological properties of TiO_2/WO_3 nanocomposite lubricants

The load carrying capacity of the TiO_2/WO_3 nanocomposite lubricant are shown in Table 5. As can be seen from Table 5, with the same amount of TBOT added, the oil film strength (P_B) is less than 147 N regardless of whether the nanoparticles are prepared under acidic or alkaline condition. Thus, it can be concluded that the tribological properties of TiO_2/WO_3 nanoparticles prepared when the concentration of TBOT is 0.01%vol are very poor, and even cannot meet the minimum value required to determine the antiwear properties of lubricating oil. However, when the TBOT concentration was increased to 0.015 vol.%, the P_B was increased by 390.74 % compared with that of 0.01 vol.% under alkaline condition. The addition of 0.015 vol.% TBOT improved the tribological properties of the prepared TiO_2/WO_3 nanoparticles.

Table 5. Results of the determination of the load carrying capacity of the lubricant.

Sample number	TBOT additions	P_B/N	D (1+5%) (mm)		
			d_1	d_2	$d_{平均}$
1	0.01vol.% pH=2	<147			
2	0.01vol.% pH=10	108	0.23	0.22	0.225
3	0.015vol.% pH=10	530	0.41	0.39	0.40

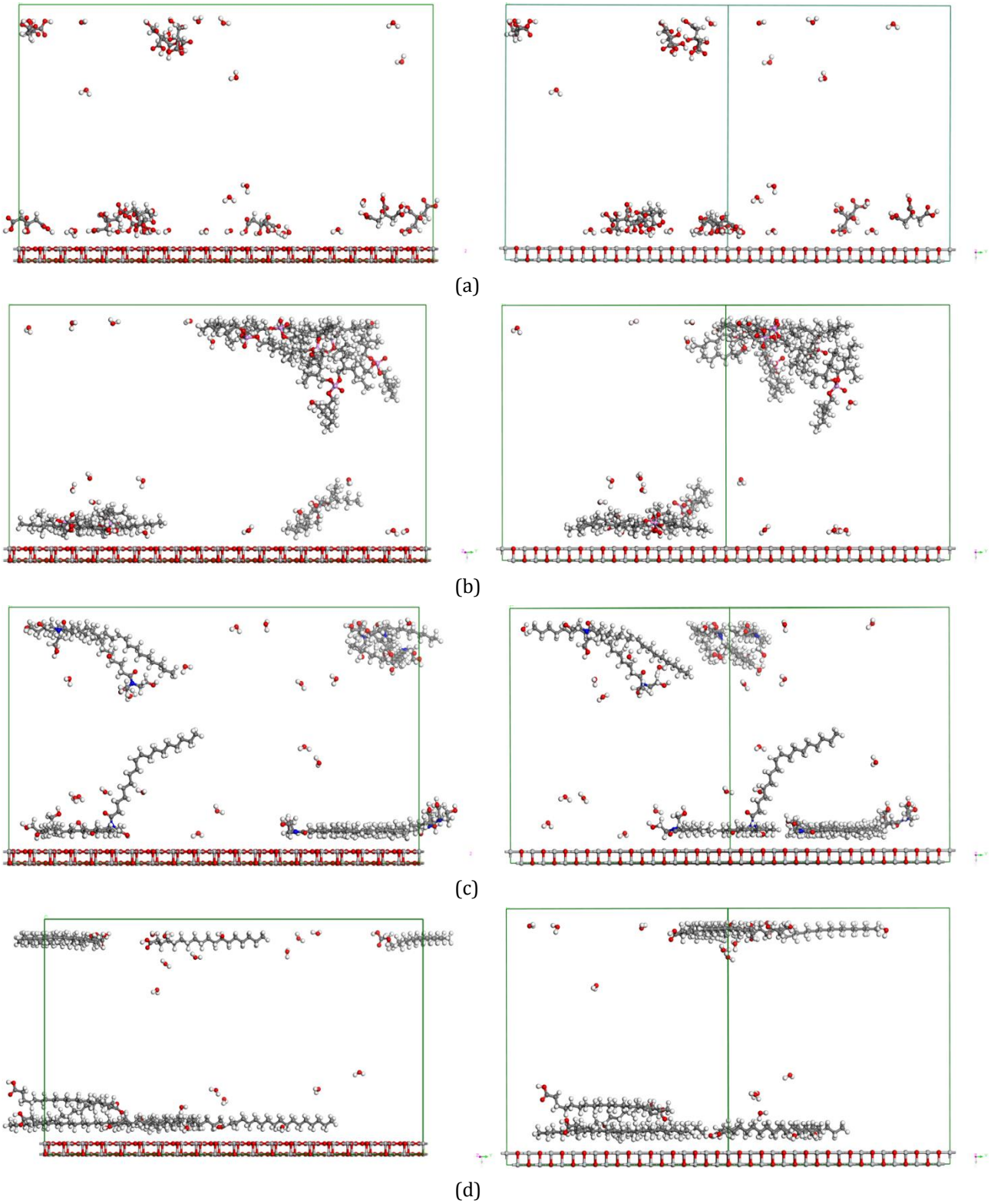

Fig. 5. Pre-adsorption (left) and pos- adsorption (right) models of the molecules on the surface of TiO_2, citric acid(a), trioctyl phosphate (b), triethanolamine oleate (c), and stearic acid(d)

Fig. 6 show coefficient of friction curve of lubricants containing TiO_2/WO_3 nanoparticle prepared with 0.01 vol.% and 0.015 vol.% TBOT under alkaline condition. It can be seen that the friction coefficient generally shows an upward trend, with more frequent and unstable fluctuations. Addition of 0.015vol.% TBOT, the friction coefficient is relatively stable and basically unchanged. Overall, when the amount of TBOT added is 0.015vol.%, the nanoparticles

have good stability, and the friction coefficient (μ = 0.087) is smaller and the wear resistance is better than that of the nanoparticles prepared with 0.01vol.% TBOT. The coefficient of friction increases from 0.06 to 0.10 in the first seconds is due to the consume of nanoparticles, and the additive may be used as a three-body material, resulting in an increase in the coefficient of friction.

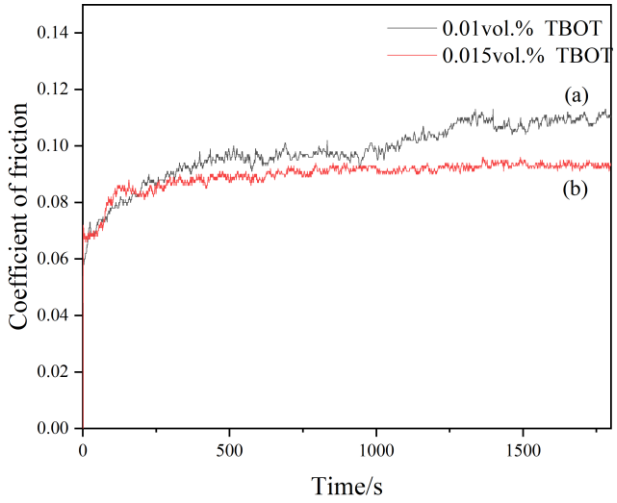

Fig. 6. Coefficient of friction curve of lubricants under alkaline condition.

3.4 Worn surface analysis

Fig. 7 shows the morphology of worn surface with lubricants after sliding. It is found that the worn surface lubricated with TiO_2/WO_3 nanoparticle prepared with 0.01 vol.% TBOT has severe wear and there are serious abrasions, pits, cracks and continuous wear marks. Compared with 0.01vol.% TBOT, the worn surface lubricated with TiO_2/WO_3 nanoparticle prepared with 0.015 vol.% TBOT is smoother and flatter, and the wear marks are lighter. When using TiO_2/WO_3 nano-composite lubricant as a lubricant, a composite lubrication film can be formed on the surface of the steel ball, which effectively alleviates the friction and wear of the contact surface. On the other hand, TiO_2-coated WO_3 nanoparticles exhibit spherical shape in microscopic morphology, spherical TiO_2/WO_3 nanoparticles as microspheres between friction pairs, which play a role of friction and wear reduction [47]. The lubrication mechanism of the TiO_2/WO_3 nano composite in the sliding process is attribute to tribofilm lubrication.

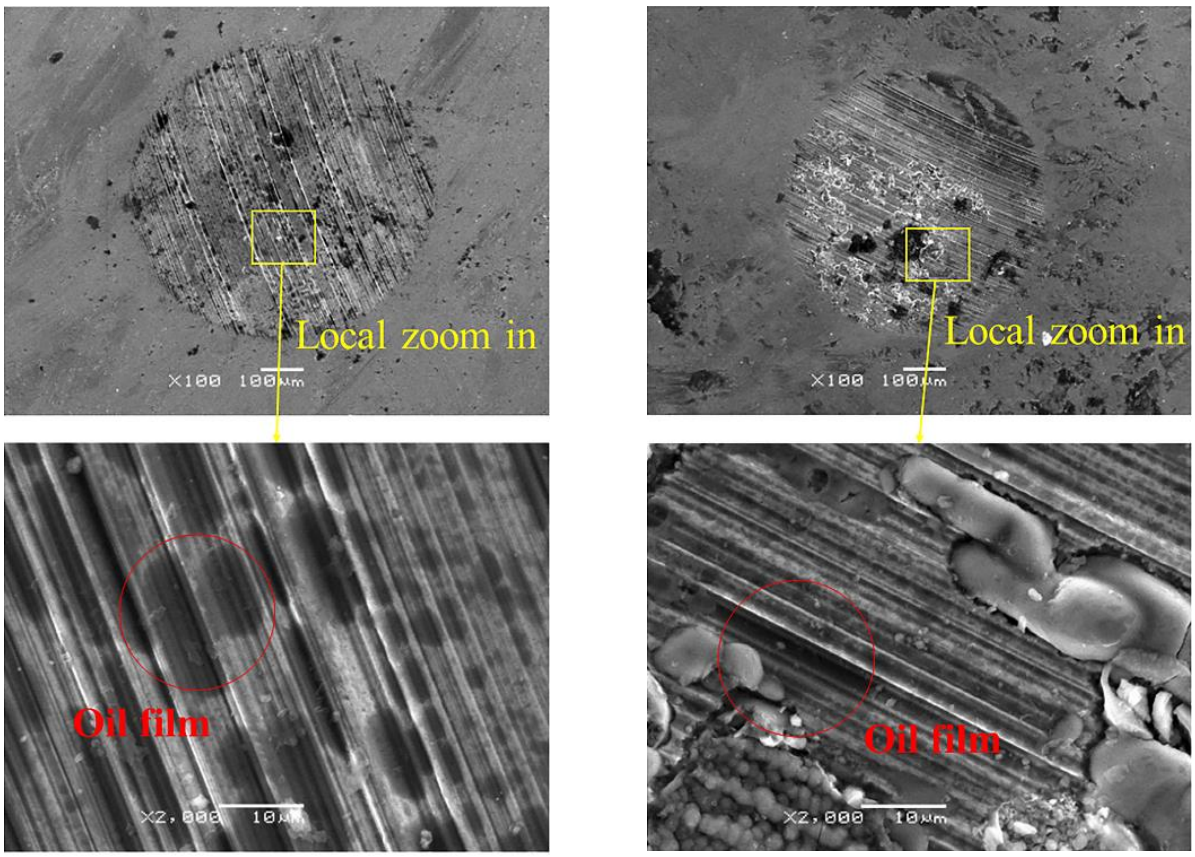

(a) (b)

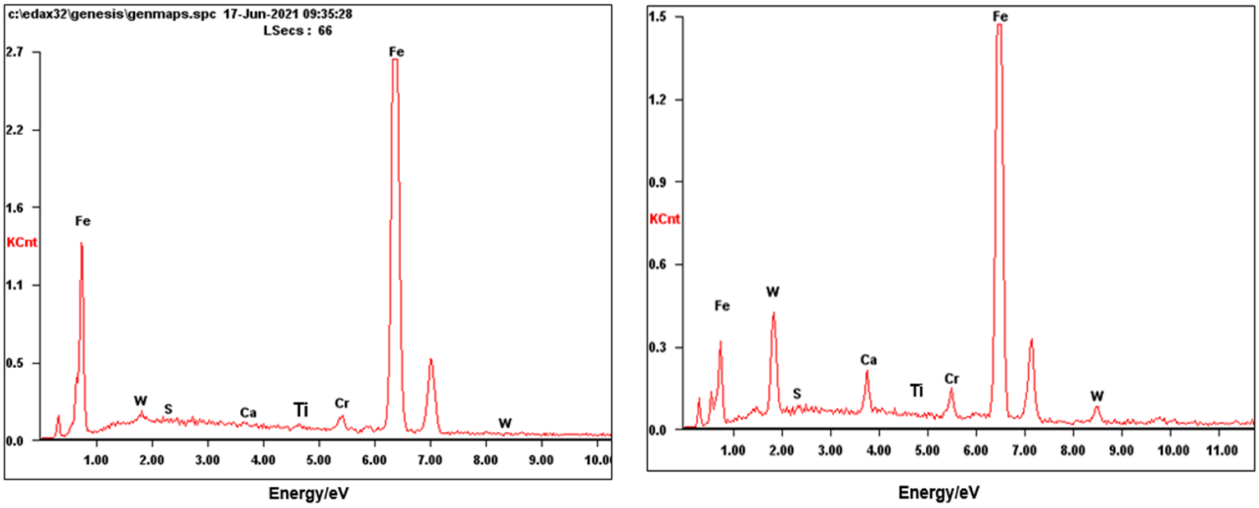

(c) (d)

Fig. 7. Morphology of the worn surface lubricated by the TiO_2@WO_3 nanoparticles prepared with (a, c) 0.015 vol.% TBOT, (b, d) 0.01vol.% TBOT.

4. CONCLUSION

WO_3 nanoparticles prepared by the sol-gel method and TiO_2/WO_3 nanocomposite particles prepared by hydrolysis process of TBOT. Microstructure and morphology of TiO_2/WO_3 nanocomposite particles was characterized by XRD and SEM. Adsorption energy between triethanolamine and TiO_2 was calculated up to -14 eV and used as a dispersant in TiO_2/WO_3 nanocomposite lubricant. Addition of 0.015 vol.% TBOT, the oil film strength is as high as 530 N, the oil film strength is increased by about 390%, the friction coefficient is 0.087. The lubrication mechanism of the TiO_2/WO_3 nano composite in the sliding process is attribute to tribofilm lubrication.

Acknowledgement

The research was supported by Jiangsu University Student Innovation and Entrepreneurship Project (202211276001Z).

REFERENCES

[1] S.N. Du, J.L. Sun, P. Wu, *Preparation Characterization and Lubrication Performances of Graphene Oxide-TiO_2 Nanofluid in Rolling Strips*, Carbon, vol. 140, pp. 338-351, 2018, doi: 10.1016/j.carbon.2018.08.055

[2] J. Qu, D.G. Bansal, B. Yu, Y. Howe Jane, H.M. Luo, S. Dai, H.Q. Li, P. J. Blau, G. Bunting Bruce, G. Mordukhovich, D.J. Smolenski, *Antiwear Performance and Mechanism of an Oil-Miscible Ionic Liquid as a Lubricant Additive,* ACS Applied Materials and Interfaces, vol. 4, iss. 2, pp. 997-1002, 2012, doi: 10.1021/am201646k

[3] A.M. Barnes, K.D. Bartle, V.R.A. Thibon, *Review of Zinc Dialkyldithiophosphates (ZDDPS): Characterisation and Role in the Lubricating Oil,* Tribology International, vol. 34, iss. 6, pp. 389-395, 2001, doi: 10.1016/S0301-679X(01)00028-7

[4] J. Zhang, H. Spikes, *On the Mechanism of ZDDP Antiwear Film Formation,* Tribology Letters, vol. 63, iss. 2, pp. 24, 2016, doi: 10.1007/s11249-016-0706-7

[5] B.T. Seymour, W.X. Fu, R.A.E. Wright, H.M. Luo, J. Qu, S. Dai, B. Zhao, *Improved Lubricating Performance by Combining Oil-Soluble Hairy Silica Nanoparticles and an Ionic Liquid as an Additive for a Synthetic Base Oil,* ACS Applied Materials and Interfaces, vol. 10, iss. 17, pp. 15129-15139, 2018, doi: 10.1021/acsami.8b01579

[6] J. Padgurskas, R. Rukuiza, I. Prosycevas, K. Raimondas, *Tribological Properties of Lubricant Additives of Fe, Cu and Co Nanoparticles,* Tribology International, vol. 60, pp. 224-232, 2013, doi: 10.1016/j.triboint.2012.10.024

[7] X.Q. Fan, W.H. Li, H.M. Fu, M.H. Zhu, L.P. Wang, Z.B. Cai, J.H. Liu, H. Li, *Probing the Function of Solid Nanoparticle Structure under Boundary Lubrication,* ACS Sustainable Chemistry and Engineering, vol. 5, iss. 5, pp. 4223-4233, 2017, doi: 10.1021/acssuschemeng.7b00213

[8] Z. Chen, X. Wen, W. Liu, S. Gunsel, J.B. Luo, *Ultrathin MoS_2 Nanosheets with Superior Extreme Pressure Property as Boundary Lubricants,* Scientific Reports, vol. 5, iss. 1, pp. 12869, 2015, doi: 10.1038/srep12869

[9] C. Shahar, D. Zbaida, L. Rapoport, H.G. Cohen, T. Bendikov, J. Tannous, F. Dassenoy, R. Tenne, *Surface Functionalization of WS_2 Fullerene-Like Nanoparticles*, Langmuir, vol. 26, iss. 6, pp. 4409-4414, 2010, doi: 10.1021/la903459t

[10] Z. Chen, X. Wen, W. Liu, S. Gunsel, J.B. Luo, *Ultrathin MoS_2 Nanosheets with Superior Extreme Pressure Property as Boundary Lubricants,* Scientific Reports, vol. 5, iss. 1, pp. 12869, 2015, doi: 10.1038/srep12869

[11] C. Shahar, D. Zbaida, L. Rapoport, H.G. Cohen, T. Bendikov, J. Tannous, F. Dassenoy, R. Tenne, *Surface Functionalization of WS_2 Fullerene-Like Nanoparticles*,Langmuir, vol. 26, iss. 6, pp. 4409-4414, 2010, doi: 10.1021/la903459t

[12] Y.W. Hu, Y.X.Wang, C.T. Wang, *One-Pot Pyrolysis Preparation of Carbon Dots as Eco- Friendly Nanoadditives of Water-Based Lubricants*, Carbon, vol. 152, pp. 511-520, 2019, doi: 10.1016/j.carbon.2019.06.047

[13] P. Saravanan, R. Selyanchyn, H. Tanaka, F.J.K. Shigenori, M.L. Stephen, S. Joichi, *Ultra-Low Friction Between Polymers and Graphene Oxide Multilayers in Nitrogen Atmosphere Mediated by Stable Transfer Film Formation*, Carbon, vol. 122, pp. 395-403, 2017, doi: 10.1016/j.carbon.2017.06.090

[14] J.F. Ou, J.Q. Wang, S. Liu, B.Mu, J.F. Ren, H.G. Wang, S.G. Yang, *Tribology Study of Reduced Graphene Oxide Sheets on Silicon Substrate Synthesized Via Covalent Assembly,* Langmuir, vol. 26, iss. 20, pp. 15830-15836, 2010, doi: 10.1021/la102862d

[15] Y.W. Hu, Y.X. Wang, Z.X. Zeng, H.C. Zhao, X.W. Ge, K. Wang, L.P. Wang, Q.J. Xue, *PEGlated Graphene as Nanoadditive for Enhancing the Tribological Properties of Water-Based Lubricant,* Carbon, vol. 137, pp. 41-48, 2018, doi: 10.1016/j.carbon.2018.05.009

[16] J.T. Robinson, J.S. Burgess, C.E. Junkermeier, *Properties of Fluorinated Graphene Films,* Nano Letters, vol. 10, iss. 8, pp. 3001-3005, 2010, doi: 10.1021/nl101437p

[17] W.X. Dai , Y. Gao, J. Huang, B.Y. Li, C. Fan, J. Yang, X.Y. Liu, *High-Yield Production of Highly Fluorinated Graphene by Direct Heating Fluorination of Graphene-Oxide,* ACS Applied Materials Interfaces, vol. 5, iss. 17, pp. 8294-8299, 2013, doi: 10.1021/am402958p

[18] R. Gusain, O.P. Khatri, *Ultrasound Assisted Shape Regulation of CuO Nanorods in Ionic Liquids and Their Use as Energy Efficient Lubricant Additives,* Journal of Materials Chemistry A, vol. 1, iss. 18, pp. 5612-5619, 2013, doi: 10.1039/C3TA10248C

[19] J. Padgurskas, R. Rukuiza, I. Prosycevas, K. Raimondas, *Tribological Properties of Lubricant Additives of Fe, Cu and Co Nanoparticles Tribo,* Tribology Intrnational, vol. 60, pp. 224-232, 2013, doi: 10.1016/j.triboint.2012.10.024

[20] X.Q. Fan, W.H. Li, H.M. Fu, M.H. Zhu, L.P. Wang, Z.B. Cai, J.H. Liu, H. Li, *Probing the Function of Solid Nanoparticle Structure under Boundary Lubrication,* ACS Sustainable Chemistry and Engineering, vol. 5, iss. 5, pp. 4223-4233, 2017, doi: 10.1021/acssuschemeng.7b00213

[21] T. Luo, X. Wei, X. Huang, H. Ling, Y. Fan, *Tribological Properties of Al_2O_3 Nanoparticles as Lubricating Oil Additives,* Ceramics International, vol. 40, iss. 5, pp. 7143-7149, 2014, doi: 10.1016/j.ceramint.2013.12.050

[22] L. Peña-Parás, J. Taha-Tijerina, L. Garza, *Effect of CuO and Al_2O_3 Nanoparticle Additives on The Tribological Behavior of Fully Formulated Oils*, Wear, vol. 332-333, pp. 1256-1261, 2015, doi: 10.1016/j.wear.2015.02.038

[23] X. Li , Z. Cao , Z.J. Zhang, H.X. Dang, *Surface-Modification in Situ of Nano-Sio_2 and Its Structure and Tribological Properties,* Applied Surface Science, vol. 252, iss. 22, pp. 7856-7861, 2006, doi: 10.1016/j.apsusc.2005.09.068

[24] M.J. Kao, C.R. Lin, *Evaluating the Role of Spherical Titanium Oxide Nanoparticles in Reducing Friction Between Two Pieces of Cast Iron, Journal of* Alloys and Compounds, vol. 483, iss. 1-2, pp. 456-459, 2009, doi: 10.1016/j.jallcom.2008.07.223

[25] A.H. Battez, J.E.F. Rico, A.N. Arias, J.L. Viesca Rodriguez, R. Chou Rodriguez, J.M. Diaz Fernandez, *The Tribological Behaviour of Zno Nanoparticles as An Additive to PAO6,* Wear, vol. 261, iss. 3-4, pp. 256-261, 2006, doi: 10.1016/j.wear.2005.10.001

[26] J. Ma, Y. Mo, M. Bai, *Effect of Ag Nanoparticles Additive on The Tribological Behavior of Multialkylated Cyclopentanes (Macs),* Wear, vol. 266, iss. 7-8, pp. 627-631, 2009, doi: 10.1016/j.wear.2008.08.006

[27] B.S. Zhang, B.S. Xu, Y. Xu, F. Gao, P.J. Shi, Y.X. Wu, *Cu Nanoparticles Effect on The Tribological Properties of Hydrosilicate Powders as Lubricant Additive for Steel-Steel Contacts. Tribol*, Int, vol. 44, iss. 7-8, pp. 878-886, 2011, doi: 10.1016/j.triboint.2011.03.002

[28] G. Hamed, B. Hasan, J. Robert, B. Michael, J. M. Khodadadi1, *The Effect of Nanoparticles on Thin Film Elasto- Hydrodynamic Lubrication,* Applied Physics Letters, vol. 103, iss. 26, 2013, doi: 10.1063/1.4858485

[29] B. Diana, N. Badri, J.C. Mathew, S.K.R.S. Subramanian, E. Ali, Z. Alexander, V.S. Anirudha, *Operando Tribochemical Formation of Onion-Likecarbon Leads to Macroscale Superlubricity,* Nature Communications, vol, 9, iss. 1, pp. 1164, 2018, doi: 10.1038/s41467-018-03549-6

[30] T. Xu, J.Z. Zhao, K. Xu, *The Ball-Bearing Effect of Diamond Nanoparticles as An Oil Additive,* Journal of Physics D: Applied Physics, vol. 29, iss. 11, pp. 2932-2937, 1996, doi: 10.1088/0022-3727/29/11/029

[31] J. Lee, S. Cho, Y.J. Hwang, C.G. Lee, S.H. Kim, *Enhancement of Lubrication Properties of Nano-Oil by Controlling the Amount of Fullerene Nanoparticle Additives,* Tribology Leterst, vol. 28, iss. 2, pp. 203-208, 2007, doi: 10.1007/s11249-007-9265-2

[32] X. Dou, A.R. Koltonow, X.L. He, J.X. Huang, *Self-Dispersed Crumpled Graphene Balls in Oil for Friction and Wear Reduction,* Proceedings of the National Academy of Sciences of the United States of America, vol. 113, iss. 6, pp. 1528-1533, 2016, doi: 10.1073/pnas.1520994113

[33] Y. Meng, F.H. Su, Y.Z. Chen, *Supercritical Fluid Synthesis and Tribological Applications of Silver Nanoparticle-Decorated Graphene in Engine Oil Nanofluid,* Scientific Reports, vol. 6, 2016, doi: 10.1038/srep31246

[34] S. Xiong, H. Wu, Z. Liu, *N-containing heterocyclic benzotriazole derivatives as new corrosion inhibitor for mild steel contained in emulsion,* Anti-Corrosion Methods And Materials, vol. 69, iss. 2, pp. 183-193, doi: 10.1108/ACMM-03-2020-2274

[35] S. Xiong, D. Liang, *Effect of sol process on structure and luminescent properties of nano-$Mn_3B7O_{13}Cl$,* Journal Of Materials Research, vol. 37, pp. 2165-2174, 2022, doi: 10.1557/s43578-022-00499-0

[36] S. Xiong, D. Liang, H. Wu, W. Lin, J.S. Chen, B.S. Zhang, *Preparation, characterization, tribological and lubrication performances of Eu doped CaWO4 nanoparticle as anti-wear additive in water-soluble fluid for steel strip during hot rolling*, Applied Surface Science, vol. 539, 2021, doi: 10.1016/j.apsusc.2020.148090

[37] S. Xiong, D. Liang, Z.X. Ba, Z. Zhang, S. Luo, *Adsorption behavior of thiadiazole derivatives as anticorrosion additives on copper oxide surface: Computational and experimental studies,* Applied Surface Science, vol. 492, pp. 399–406, 2019, doi: 10.1016/j.apsusc.2019.06.253

[38] S. Xiong, D. Liang, Z.W. Zhao, *Effects of lubricants and nano-inclusions on copper corrosion behavior and their electrical conductivity,* Journal of Electronic Materials, vol. 47, iss. 8, pp. 4694-4702, 2018, doi: 10.1007/s11664-018-6341-3

[39] H.M. Xie, B. Jiang, J.J. He, X.S. Xia, F.S. Pan, *Lubrication Performance of MoS_2 and SiO_2 Nanoparticles as Lubricant Additives in Magnesium Alloy-steel Contacts*, Tribology International, vol. 93, pp. 63–70, 2016, doi: 10.1016/j.triboint.2015.08.009

[40] W.J. Zhao, X.J. Ci, *TiO_2 Nanoparticle/ Fluorinated Reduced Graphene Oxide Nanosheet Composites for Lubrication and Wear Resistance*, ACS Applied Nano Materials, vol. 3, iss. 9, pp. 8732-8741, 2020, doi: 10.1021/acsanm.0c01547

[41] Y. Meng, F.H. Su, Y.Z. Chen, *Au/Graphene Oxide Nanocomposite Synthesized in Supercritical CO_2 Fluid as Energy Efficient Lubricant Additive*, ACS Applied Materials and Interfaces, vol. 9, pp. 39549-39559, 2017, doi: 10.1021/acsami.7b10276

[42] S.Q. Huang, A.S. He, J.H. Yun, X.F. Xu, Z.Y. Jiang, S.H. Jiao, H. Huang, *Synergistic Tribological Performance of a Water Based Lubricant Using Graphene Oxide and Alumina Hybrid Nanoparticles as Additives*, Tribology International, vol. 135, pp. 170-180, 2019, doi: 10.1016/j.triboint.2019.02.031

[43] W.M. Liu, Y.X. Chen, G.T. Kou, T. Xu, D.C. Sun, *Characterization and Mechanical/Tribological Properties of Nano Au-TiO_2 Composite Thin Films Prepared by a Sol-Gel Process*, Wear, vol. 254, iss. 10, pp. 994-1000, 2003, doi: 10.1016/S0043-1648(03)00305-3

[44] M. Kasiarova, E. Rudnayova, J. Dusza, M. Hnatko, P. Sajgalik, A. Merstallinger, L. Kuzsella, *Some Tribological Properties of a Carbon-Derived Si_3N_4/SiC Nanocomposite*, Journal of the European Ceramic Society, vol. 24, iss. 12, pp. 3431-3435, 2004, doi: 10.1016/j.jeurceramsoc.2003.10.029

[45] P. Bhimaraj, D. Burris, W.G. Sawyer, C.G. Toney, R.W. Siegel, L.S. Schadler, *Tribological In-Vestigation of The Effects of Particle Size, Loading and Crystal-Linity on Poly(Ethylene) Terephthalate Nanocomposites*, Wear, vol. 264, iss. 8, pp. 632-637, 2008, doi: 10.1016/j.wear.2007.05.009

[46] S. Xiong, X.M. Zhang, D. Liang, *Preparation, microstructure and luminescence properties of TiO2/WO3 composites*, Applied Physics A-Materials Science & Processing, vol. 128, iss. 9, pp. 778, 2022, doi: 10.1007/s00339-022-05920-3

[47] Y.X. Wu, W. Li, M. Zhang, X.B. Wang, *Oxidative Degradation of Synthetic Ester and Its Influence on Tribological Behavior*, Tribology International, vol. 64, iss. 3, pp. 16-23, 2013, doi: 10.1016/j.triboint.2013.02.002